NEW OBSERVATIONS OF THE ABSORPTION SPECTRUM OF PKS 0237−23 AND THEIR IMPLICATIONS FOR THE ORIGIN OF QUASAR ABSORPTION LINES

TODD BOROSON AND WALLACE L. W. SARGENT

Hale Observatories, California Institute of Technology, Carnegie Institution of Washington

AND

A. BOKSENBERG AND R. F. CARSWELL

Department of Physics and Astronomy, University College London

ABSTRACT

The QSO PKS 0237−23 has been observed with the University College London image photon-counting system (IPCS) at the coudé focus of the Hale telescope. Six observations made over 3 years have been combined to give high-resolution (0.7 Å) spectral coverage from $\lambda 3700$ to $\lambda 4300$. Wavelengths and equivalent widths of 193 absorption lines in this spectral region have been tabulated. Most of the lines are identified in 45 redshift systems based on C IV doublets. Eleven of these have been labeled "certain," 12 have been labeled "probable," and 22 have been called "possible." A large statistical excess of these systems shows the Si II $\lambda 1533$ excited fine-structure transition.

The 45 C IV doublets have a nonuniform distribution in redshift; this nonuniformity is apparently caused by a peak at $z \sim 1.65$ with a width of 5000 km s^{-1}. An analysis of the splittings between C IV redshifts shows an excess of small splittings, $\Delta v \approx 150$ km s^{-1}, and an excess at $\Delta v \approx 1800$ km s^{-1}. The excess of small splittings may be due to a continuum of splittings less than $\Delta v \sim 200$ km s^{-1}. If the other peak is due to absorption-line locking, the only line pair which could account for it comprises Lβ and O VI $\lambda 1031$. The implications of absorption systems with $z_{em} - z_{abs} \geqslant 0.5$ which show excited fine-structure lines are discussed in terms of the origin of the systems.

Subject headings: line identifications — quasars

I. INTRODUCTION

The QSO PKS 0237−23 is one of the best-studied and most poorly understood absorption-line quasi-stellar objects. It was identified as a QSO by Arp, Bolton, and Kinman (1967), who found an emission redshift of 2.22. The rich absorption spectrum has been studied in detail by several groups, most recently by Boksenberg and Sargent (1975, and references therein). They obtained high-resolution data by using the University College London image photon-counting system (IPCS) at the coudé focus of the Hale telescope in 1973 October. They found 75 absorption lines in the wavelength region $\lambda 3700$ to $\lambda 4300$, and, combining these with 26 lines observed in previous studies outside this region, they identified 19 certain redshift systems, three possible systems, and three doubtful systems. One-fifth of the lines, some of them quite strong, were not identified.

Boksenberg and Sargent found that several of the previously identified systems were actually two or more systems split by a small amount. Furthermore, two values of this splitting seemed to occur more frequently than could be accounted for by chance. Four splittings equivalent to the C IV resonance doublet $\lambda 1548.20$, $\lambda 1550.77$ (500 km s^{-1}), and seven splittings of $\Delta z = 0.0012$ (141 km s^{-1}), were found. The split-

tings corresponding to the C IV doublet were given as possible evidence of absorption-line locking, an effect which may occur if the absorption regions are being radiatively accelerated by the QSO. The smaller splitting was not explained by Boksenberg and Sargent. Bahcall (1975) showed that the many occurrences of this splitting could be an illusion produced by a continuum of splittings most of which were smaller than the resolution of the instrument.

PKS 0237−23 was observed again with the IPCS in 1974 October and 1975 November at the coudé focus of the Hale telescope. These observations have been combined with the older data in order to obtain new high-resolution spectra with better signal-to-noise ratios. In § II, these observations and the initial data reduction are described. Section III is concerned with the identification of redshift systems in the spectra; § IV discusses the new redshift systems and evidence for their reality. Section V deals with physical implications of the new systems. In § VI, we conclude with a summary of the major points.

II. OBSERVATIONS AND INITIAL DATA REDUCTION

The University College London IPCS has been described by Boksenberg and Sargent (1975, and references therein). In all, six separate observations

772

TABLE 1

IPCS OBSERVATIONS OF PKS 0237−23

Date	Runs	Wavelength Range Covered	Average Dispersion (Å/ch.)	Length of Exposure (hr)
1973 Oct......	69–70	λ3700–λ4000	0.31	2.0
1973 Oct......	67–68	4000– 4300	0.31	1.5
1974 Oct......	101–104	3700– 4000	0.31	2.0
1975 Nov.....	6–9	4000– 4300	0.31	1.2
1975 Nov.....	69–74	4000– 4165	0.16	2.0
1975 Nov.....	112–116	4000– 4165	0.16	2.0

were incorporated in this study, covering wavelengths from λ3700 to λ4300. In each observation, the sky was subtracted from the object plus sky signal. The parameters of these observations are presented in Table 1. In all observations the projected slit width was two channels. Before or after each exposure, a hollow cathode Ar-Fe arc was observed. A fifth-order polynomial was fitted to the dispersion of each arc spectrum, and each observation was divided into channels 0.25 Å or 0.125 Å wide, depending on the original dispersion. All of these were then added to obtain a spectrum with 0.25 Å wide channels. The existence of different amounts of data at different wavelengths caused several discontinuities in the continuum level.

These were removed by multiplying each point by a corrective factor. The resulting spectrum is shown in Figures 1 and 2. Figure 3 shows the continuum level as a function of wavelength as it appeared before adjustment. The vertical axis is real counts, and therefore the uncertainties in any channel are the square root of the counts per channel at that point.

The list of lines, Table 2, was constructed from the spectrum by requiring that any line extend more than 3 standard deviations below the real continuum level and have a width of at least two channels. An attempt was made to separate obviously blended lines which were incompletely resolved. The wavelength and equivalent width of each line were measured; these
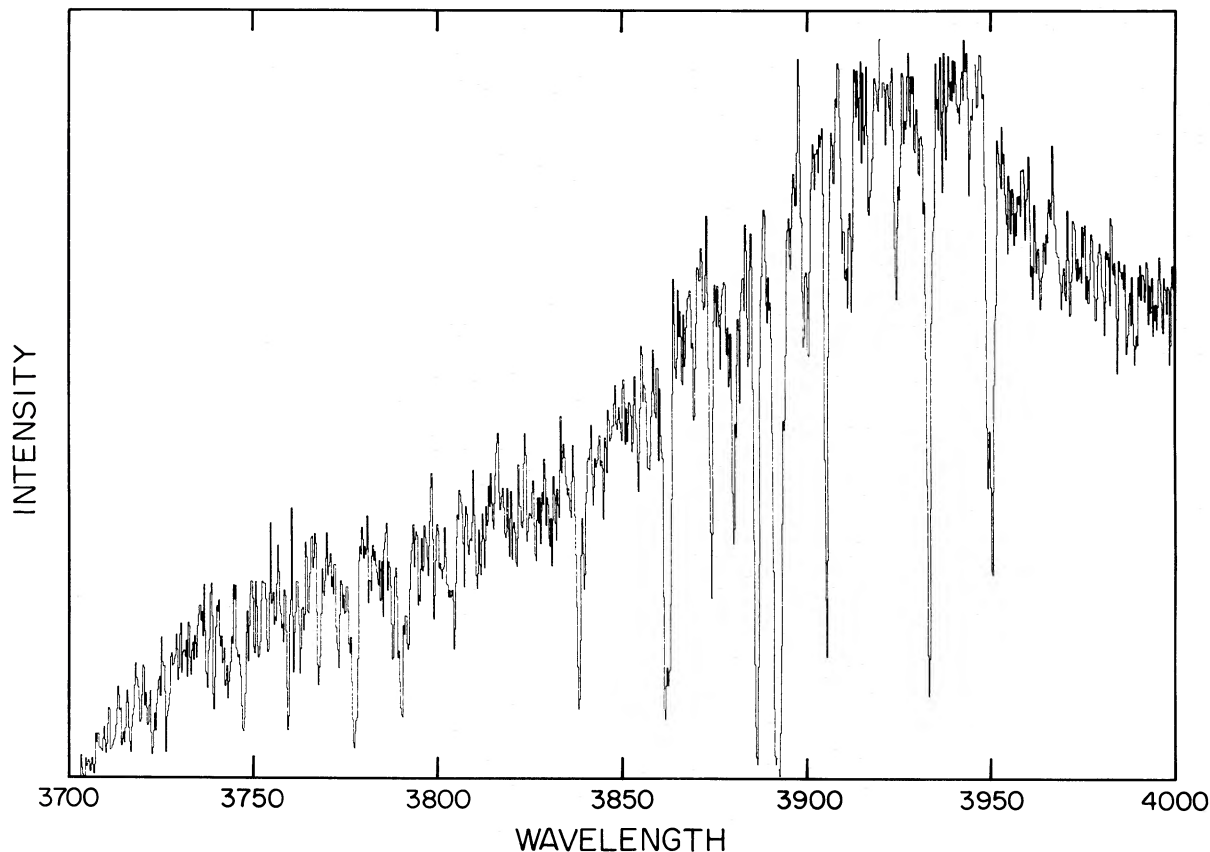
FIG. 1.—The spectrum of PKS 0237−23 in the wavelength region λλ3700–4000. The peak at λ3930 is Lα emission.
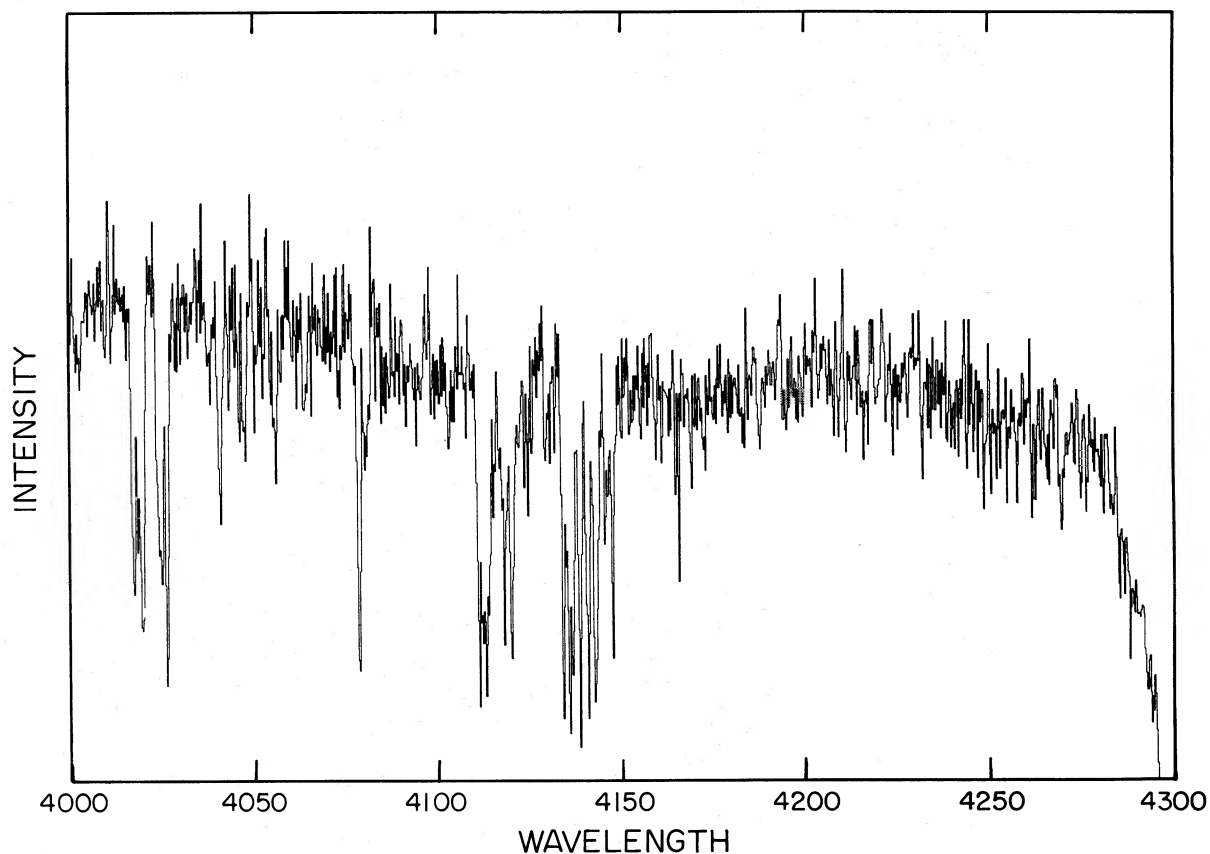
FIG. 2.—The spectrum of PKS 0237−23 in the wavelength region λλ4000–4300

are given in Table 2. The line list contains 193 lines between λ3700 and λ4300. All lines with equivalent widths of 0.2 Å or greater are certainly real; some of those with equivalent widths of 0.1 Å may be noise. We find about 2½ times as many lines as Boksenberg and Sargent found in the same region of the spectrum.

Most of the new lines are weak ones; all the lines found by Boksenberg and Sargent with intensities greater than zero on their arbitrary scale occur in the new data as strong lines. We estimate that the measured equivalent widths of the strong lines are accurate to about 20%, while those of the weak lines are accurate
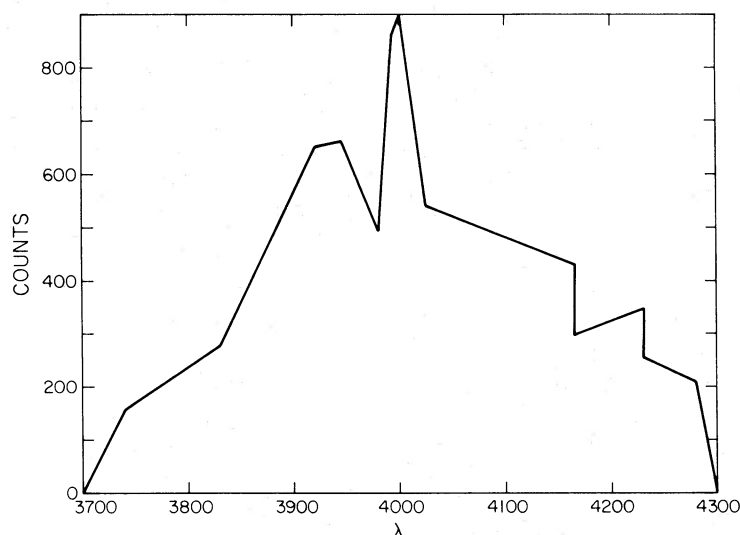
FIG. 3.—The number of counts per channel (0.25 Å) as a function of wavelength for the data in Figs. 1 and 2

TABLE 2

ABSORPTION LINES IN PKS 0237−23 FROM IPCS DATA

Wavelength (Å)	Equivalent Width (Å)	Wavelength (Å)	Equivalent Width (Å)	Wavelength (Å)	Equivalent Width (Å)	Wavelength (Å)	Equivalent Width (Å)
3716.9	0.6	3979.1	0.2	4024.3	0.3	4125.7	0.1
3721.7	0.3	3880.3	0.7	4025.1	1.2	4129.5	0.3
3722.8	0.9	3882.0	0.1	4026.3	0.8	4130.7	0.1
3726.5	0.9	3884.3	0.2	4029.0	0.1	4132.0	0.1
3737.8	0.5	3886.7	1.9	4030.4	0.1	4134.2	0.9
3739.4	0.6	3889.5	0.1	4032.4	0.1	4135.0	0.3
3741.9	0.2	3891.8	0.9	4037.6	0.1	4135.9	0.9
3742.6	0.3	3892.2	1.2	4038.4	0.1	4136.7	0.8
3743.3	0.5	3892.8	0.8	4041.0	0.6	4138.7	0.8
3746.0	0.1	3894.1	0.4	4043.4	0.1	4141.0	1.1
3747.4	1.1	3899.3	0.3	4046.4	0.2	4142.7	1.4
3748.8	0.2	3900.7	0.3	4047.8	0.4	4145.5	0.4
3750.3	0.2	3905.5	0.9	4050.6	0.1	4146.3	0.3
3751.6	0.4	3909.8	0.1	4052.6	0.1	4147.7	0.5
3754.2	0.4	3910.8	0.2	4054.8	0.1	4150.0	0.1
3758.3	0.2	3911.4	0.2	4056.1	0.3	4152.1	0.1
3759.6	0.8	3912.4	0.2	4057.6	0.1	4155.3	0.1
3761.1	0.3	3917.1	0.2	4060.8	0.1	4159.3	0.2
3762.8	0.3	3924.6	0.3	4063.8	0.4	4160.8	0.1
3763.8	0.2	3925.4	0.1	4064.4	0.1	4164.5	0.2
3767.8	0.8	3930.8	0.1	4073.4	0.1	4165.6	0.3
3773.3	0.5	3933.4	1.3	4078.6	1.1	4169.0	0.2
3776.3	0.2	3937.2	0.1	4080.4	0.3	4172.8	0.1
3777.5	1.8	3944.4	0.1	4080.9	0.2	4187.8	0.2
3788.0	0.5	3949.5	0.7	4081.7	0.2	4208.1	0.2
3789.2	0.1	3950.6	1.0	4087.2	0.2	4209.3	0.2
3790.6	1.1	3954.9	0.1	4088.7	0.1	4211.4	0.2
3792.3	0.5	3955.7	0.1	4091.7	0.1	4216.1	0.2
3795.1	0.2	3957.0	0.1	4093.9	0.1	4217.4	0.1
3799.2	0.3	3959.7	0.1	4094.5	0.1	4222.1	0.1
3803.6	0.3	3961.7	0.2	4095.7	0.2	4224.1	0.1
3804.7	0.5	3963.7	0.2	4098.5	0.1	4225.3	0.1
3807.4	0.1	3969.4	0.1	4100.7	0.1	4228.1	0.1
3810.9	0.3	3970.6	0.1	4103.2	0.3	4232.1	0.2
3811.9	0.1	3971.8	0.1	4104.5	0.1	4244.2	0.2
3821.7	0.1	3978.9	0.1	4108.0	0.2	4247.1	0.1
3826.9	0.1	3981.3	0.1	4111.4	0.9	4248.6	0.2
3831.2	0.1	3984.7	0.1	4111.9	0.4	4250.6	0.1
3838.5	1.2	3987.3	0.1	4112.4	0.4	4254.9	0.1
3840.0	0.5	3989.4	0.1	4113.2	0.9	4257.6	0.1
3842.5	0.1	3992.3	0.1	4113.9	0.6	4261.6	0.2
3845.2	0.1	3999.0	0.1	4115.2	0.4	4262.6	0.1
3854.4	0.3	4001.9	0.2	4116.9	0.2	4269.7	0.2
3857.3	0.3	4002.9	0.3	4117.7	0.2	4285.4	0.3
3861.7	1.4	4009.9	0.2	4118.2	0.7	4286.7	0.2
3862.6	0.8	4011.4	0.2	4120.2	1.1	4288.1	0.3
3869.7	0.2	4017.6	0.7	4122.2	0.2		
3874.2	0.7	4018.6	0.4	4123.7	0.2		
3876.8	0.1	4019.8	1.2	4124.8	0.2		

to about 0.1 Å. The wavelengths of the lines are probably accurate to 0.3 Å except in the case of blended lines, where the error may be twice as large.

III. THE REDSHIFT DETERMINATIONS

There are certain basic problems in identifying the lines in a spectrum such as that of PKS 0237−23. First, the high-resolution data cover only a small part of the spectrum, in the rest frame of the absorbing region, only $1/(1 + z) \sim \frac{1}{3}$ of the range of the observed data. The rest wavelengths of commonly seen or expected lines fall between $\lambda 900$ and $\lambda 3000$; very few of these occur in any 200 Å interval. Second, while the IPCS data are accurate in wavelength to several

tenths of an angstrom and lines with equivalent widths down to 0.1 Å are measurable, most of the data from outside the well-observed region are of very poor quality. We estimate that all lines shortward of $\lambda 3700$ or longward of $\lambda 4300$ that were included by Boksenberg and Sargent have equivalent widths greater than 1 angstrom and positions accurate to only 2 or 3 angstroms. A third problem is that, in any rich QSO absorption spectrum, there is a significant probability of finding a line near any point picked at random. Thus a certain number of systems can be expected to identify several lines by chance alone.

In previous studies, two methods have been used for identifying redshift systems. In spectra containing a small number of lines and covering a large wave-

length region, it is fairly straightforward to identify the strong observed lines with resonance transitions of the cosmically abundant elements. With high-resolution observations of rich spectra, however, the density of lines becomes so great that a significant probability of chance identification exists. The reality of systems found in rich spectra has been appraised by comparing the appearance of these systems with the most believable systems found in "nonsense spectra," generated with random numbers. A more complex version of this method was used by Aaronson, McKee, and Weisheit (1975), who wrote a computer code which checks the physical consistency of identified lines automatically, and is thus able to analyze hundreds of "nonsense spectra" with exactly the same criteria as the real spectrum.

Clearly, because of the complexity of the spectrum of PKS 0237−23, none of these methods could produce completely satisfactory results. In our data, there is approximately a one-fourth chance of finding a line at any point chosen at random within a $\Delta\lambda$ of 0.3 Å, and, with only five or six lines accessible at any redshift, one can easily calculate that dozens of systems will arise by chance; obviously, though, there are many real systems. As a first effort toward identifying the lines, we binned the spectrum in channels of constant $\Delta\lambda/\lambda = 10^{-4}$ and calculated the autocorrelation function

$$A(n) = \sum_{i=1}^{m} S(i)S(i + n),$$

where $S(i)$ is the number of counts in the ith channel, m is the number of channels, and n is the shift in channels. This is shown in Figure 4, in which the shift plotted is $1 + \Delta\lambda/\lambda$. Any doublet or closely

spaced lines which occur in several redshift systems will appear as a peak in the autocorrelation function at a shift corresponding to the ratio of the wavelengths. Twenty-six peaks appear in the autocorrelation function with shifts between 1.00 and 1.05. When the positions of these peaks were compared with ratios of the 38 "lines most likely to succeed" given by Bahcall (1968), seven were found to correspond, within 10^{-4}, to the following ratios: C IV $\lambda1548.20$, $\lambda1550.77$; N V $\lambda1238.82$, $\lambda1248.80$; Si II $\lambda1526.72$, $\lambda1533.44$; H I $\lambda1215.67$, N V $\lambda1238.82$; H I (Lδ) $\lambda949.74$, C III $\lambda977.03$; Si III $\lambda1206.51$; N V $\lambda1248.80$; and Si III $\lambda1206.51$, Si II $\lambda1260.42$. The identifications of the peaks indicate that a considerable portion of the visible lines must be identified with two wavelength regions in the rest frame, one around the C IV doublet and one around Lα. This result is not surprising; these are the two strongest features in most QSO absorption spectra, and it might be expected that whenever they are accessible they will produce the strongest peaks in the autocorrelation function. Two searches were performed, one for the C IV doublet $\lambda\lambda1548$, 1550 and the Si II lines $\lambda1526.72$ and $\lambda1533.44$, the other for Lα, N V $\lambda1238.82$, $\lambda1242.80$, the Si III line $\lambda1206.51$, and the strong Si II lines $\lambda1193.28$, $\lambda1260.42$, $\lambda1190.42$, and $\lambda1304.37$.

The C IV doublet played an important role in the identifications of several redshift systems found by Boksenberg and Sargent. Eight of their 19 certain systems contain only the C IV doublet and one or both of the Si II lines $\lambda\lambda1526$, 1533. It is, therefore, reasonable to expect more systems of this type to appear in the new data. The search for such systems was conducted as follows: Line pairs identified as C IV doublets were required to have the correct separation to ±0.3 angstroms. The ratio of the
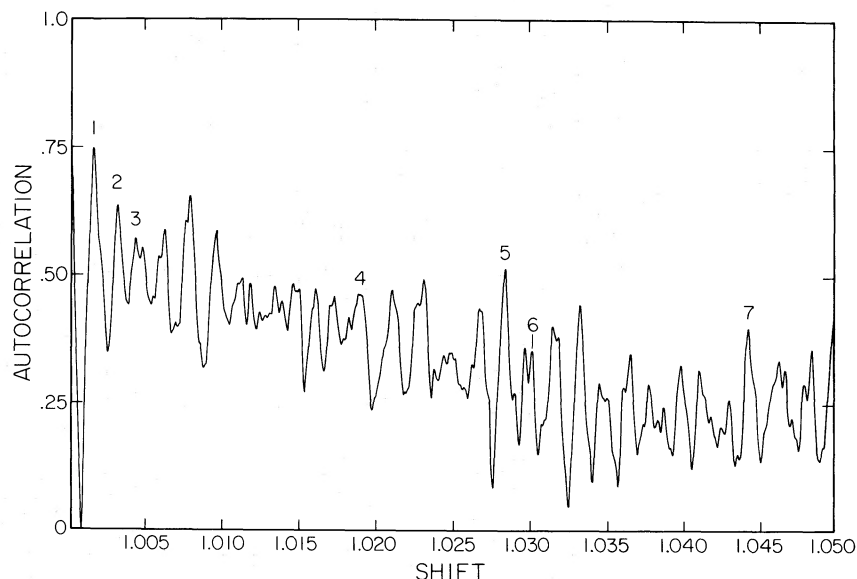
FIG. 4.—The autocorrelation function of the spectrum of PKS 0237−23. The vertical scale is arbitrary; the horizontal scale is a measure of the lag $1 + \Delta\lambda/\lambda$ introduced in calculating the autocorrelation. The seven numbered peaks correspond to the seven line ratios given in the text.

equivalent widths $W(\lambda1548):W(\lambda1548)$ should lie between 2 and 1. This requirement was made with appropriate account taken of the accuracy of the equivalent widths. Occasional exceptions were made to this constraint if one of the lines was obviously an unresolved blend. Forty-five possible C IV doublets emerged from this search, and these are presented in Table 3. For each of these doublets, the two Si II lines, $\lambda1526.72$, $\lambda1533.44$, and, where accessible, the Si IV doublet, $\lambda1393.76$, $\lambda1402.77$, were looked for within a $\Delta\lambda$ of 0.3 Å. The resulting additional identifications for 39 of the C IV systems are presented in Table 4, with some identifications of lines outside the IPCS wavelength region. These additional lines are taken from the line list in Boksenberg and Sargent (1975), and identifications of these lines were required

to be accurate only to several angstroms. The 45 C IV redshift systems identify 106 of the 193 lines in the spectrum, including 57 of the 80 lines between $\lambda4000$ and $\lambda4200$.

The C IV systems leave about 90 lines unidentified, most of them shortward of the Lα emission line. An attempt was made to identify these with Lα, the N V $\lambda\lambda1238$, 1242 doublet, the Si III $\lambda1206$ line, and the Si II lines $\lambda\lambda1190$, 1193, 1260, 1304. No system identified all accessible wavelengths, and no method could be determined to convincingly separate the real systems from the chance identifications. We think that it is likely that the strong unidentified absorption lines shortward of the Lα emission line are Lα at different redshifts, and that the weaker lines are N V, Si II, and Si III at some of these redshifts. However, we

TABLE 3
C IV Doublets in PKS 0237−23

| | C IV 1548.20 | | C IV 1550.77 | | |
| | Wavelength (Å) | Equivalent Width (Å) | Wavelength (Å) | Equivalent Width (Å) | |
z					Reality
1.4007.....	3716.9	0.6	3722.8	0.9	PO
1.4174.....	3742.6	0.3	3748.8	0.2	PO
1.4575.....	3804.7	0.5	3810.9	0.3	PO
1.5023.....	3874.2	0.7	3880.3	0.7	C
1.5144.....	3892.8	0.8	3899.3	0.3	PR
1.5153.....	3894.1	0.4	3900.7	0.3	PR
1.5260.....	3910.8	0.2	3917.1	0.2	PO
1.5348.....	3924.6	0.3	3930.8	0.1	PR
1.5389.....	3930.8	0.1	3937.2	0.1	PO
1.5546.....	3954.9	0.1	3961.7	0.2	PO
1.5559.....	3957.0	0.1	3963.7	0.2	PR
1.5603.....	3963.7	0.2	3970.6	0.1	PR
1.5950.....	4017.6	0.7	4024.3	0.3	C
1.5964.....	4019.8	1.2	4026.3	0.8	C
1.6102.....	4041.0	0.6	4047.8	0.4	C
1.6146.....	4047.8	0.4	4054.8	0.1	PO
1.6164.....	4050.6	0.1	4057.6	0.1	PO
1.6209.....	4057.6	0.1	4064.4	0.1	PO
1.6311.....	4073.4	0.1	4080.4	0.3	PO
1.6356.....	4080.4	0.3	4087.2	0.2	PR
1.6365.....	4081.7	0.2	4088.7	0.1	PR
1.6399.....	4087.2	0.2	4093.9	0.1	PR
1.6410.....	4088.7	0.1	4095.7	0.2	PO
1.6429.....	4091.7	0.1	4098.5	0.1	PO
1.6443.....	4093.9	0.1	4100.7	0.1	PO
1.6512.....	4104.5	0.1	4111.4	0.9	PO
1.6556.....	4111.4	0.9	4118.2	0.7	C
1.6568.....	4113.2	0.9	4120.2	1.1	C
1.6581.....	4115.2	0.4	4122.2	0.2	C
1.6591.....	4116.9	0.2	4123.7	0.2	PO
1.6598.....	4117.7	0.2	4124.8	0.2	PR
1.6599.....	4118.2	0.7	4124.8	0.2	PR
1.6636.....	4123.7	0.2	4130.7	0.1	PO
1.6703.....	4134.2	0.9	4141.0	1.1	C
1.6714.....	4135.9	0.9	4142.7	1.4	C
1.6732.....	4138.7	0.8	4145.5	0.4	C
1.6747.....	4141.0	1.1	4147.7	0.5	C
1.6775.....	4145.5	0.4	4152.1	0.1	PO
1.6820.....	4152.1	0.1	4159.3	0.2	PR
1.6907.....	4165.6	0.3	4172.8	0.1	PR
1.7188.....	4209.3	0.2	4216.1	0.2	PO
1.7240.....	4217.4	0.1	4224.1	0.1	PO
1.7292.....	4225.3	0.1	4232.1	0.2	PO
1.7455.....	4250.6	0.1	4257.6	0.1	PO
1.7533.....	4262.6	0.1	4269.7	0.2	PO

TABLE 4

FURTHER IDENTIFICATIONS IN C IV DOUBLET REDSHIFT SYSTEMS

z	Ion	Rest Wavelength Å	Observed Wavelength Å	Equivalent Width*	z	Ion	Rest Wavelength Å	Observed Wavelength Å	Equivalent Width*
1.4007	C II	1334.50	3205.70	(7)	1.6568	Si II	1260.42	3347.35	(4)
	Si IV	1393.76	3347.35	(4)		Si IV	1393.76	3803.27	(2)
	Si IV	1402.77	3364.70	(2)		Si IV	1402.77	3726.5	0.9
	Si II	1526.72	3667.00	(4)		Si II	1526.72	4056.1	0.3
1.4575	C II	1334.50	3281.00	(6)	1.6581	Si II	1260.42	3347.35	(4)
	Si IV	1402.77	3445.01	(3)		Si IV	1393.76	3703.27	(2)
	Si II	1526.72	3751.6	0.4	1.6591	Si IV	1393.76	3703.27	(2)
1.5144	C II	1334.50	3354.90	(3)	1.6598	Si II	1260.42	3354.90	(3)
	Si IV	1393.76	3501.23	(4)		Si II	1526.72	4060.8	0.1
	Si IV	1402.77	3525.07	(4)		Si II	1533.44	4078.9	1.1
	Si II	1526.72	3838.5	1.2	1.6599	Si II	1260.42	3354.90	(3)
1.5153	C II	1334.50	3354.90	(3)		Si II	1526.72	4060.8	0.1
	Si II	1526.72	3840.0	0.5		Si II	1533.44	4078.9	1.1
	Si II	1533.44	3857.3	0.3	1.6636	Si II	1260.42	3354.90	(3)
1.5348	Si IV	1402.77	3555.00	(2)		C II	1334.50	3555.00	(2)
	Si II	1526.72	3869.7	0.2	1.6703	Si II	1260.42	3364.70	(2)
	Si II	1533.44	3886.7	1.9		C II	1334.50	3565.10	(2)
1.5546	Si II	1533.44	3917.1	0.2		Si IV	1393.76	3721.7	0.3
1.5559	Si IV	1393.76	3565.10	(2)		Si IV	1402.77	3746.0	0.1
1.5603	Si IV	1393.76	3565.10	(2)		Si II	1533.44	4094.5	0.1
	Si IV	1402.77	3592.77	(3)	1.6714	Si II	1260.42	3364.70	(2)
1.5950	Si II	1526.72	3961.7	0.2		C II	1334.50	3565.10	(2)
1.5964	Si II	1526.72	3963.7	0.2		Si IV	1402.77	3747.4	1.1
	Si II	1533.44	3981.3	0.1		Si II	1526.72	4078.6	1.1
1.6102	Si IV	1402.77	3660.20	(4)	1.6732	H I	1215.67	3251.10	(8)
	Si II	1526.72	3984.7	0.1		C II	1334.50	3565.10	(2)
	Si II	1533.44	4002.9	0.3		Si II	1526.72	4080.9	0.2
1.6146	Si IV	1402.77	3667.00	(4)	1.6747	H I	1215.67	3251.10	(8)
1.6164	Si IV	1402.77	3667.00	(4)	1.6775	C II	1334.50	3571.80	(3)
1.6211	Si IV	1393.76	3667.00	(4)	1.6820	Si IV	1393.76	3737.8	0.5
1.6356	H I	1215.67	3205.70	(7)		Si II	1526.72	4094.5	0.1
	Si IV	1402.77	3695.80	(3)		Si II	1533.44	4112.4	0.4
1.6365	H I	1215.67	3205.70	(7)	1.6907	C II	1334.50	3592.77	(3)
	Si IV	1402.77	3695.80	(3)		Si IV	1393.76	3750.3	0.2
	Si IV	1526.72	4025.1	(1.2)		Si II	1526.72	4108.0	0.2
1.6399	C II	1334.50	3525.07	(4)		Si II	1533.44	4125.7	0.1
	Si IV	1402.77	3703.27	(2)	1.7188	Si IV	1393.76	3789.2	0.1
	Si II	1526.72	4030.4	0.1		Si II	1533.44	4169.0	0.2
	Si II	1533.44	4047.8	0.4	1.7292	Si IV	1393.76	3803.6	0.3
1.6410	C II	1334.50	3525.07	(4)	1.7455	Si IV	1393.76	3826.9	0.1
	Si IV	1402.77	3703.27	(2)	1.7533	H I	1215.67	3347.35	(4)
	Si II	1526.72	4032.4	0.4		Si II	1533.44	4222.1	0.1
1.6429	C II	1334.50	3525.07	(4)					
	Si IV	1393.76	3685.45	(1)					
	Si II	1533.44	4052.6	0.1					
1.6443	Si IV	1393.76	3685.45	(1)					
	Si II	1533.44	4054.8	0.1					
1.6512	Si IV	1393.76	3695.80	(3)					
	Si II	1526.72	4047.8	0.4					
1.6556	Si II	1260.42	3347.35	(4)					
	Si IV	1393.76	3703.27	(2)					

*Numbers in parentheses are subjective intensities for lines found in previous work; other numbers are equivalent widths in angstroms.

cannot confirm the reality of any of these redshifts individually except the two systems found by Boksenberg and Sargent, who used lines measured in earlier studies, $z = 2.1758$ and $z = 2.2013$. For this reason, the analysis of statistical and physical properties of the redshift systems will pertain only to the C IV systems which can be found in our data between redshifts of 1.40 and 1.76.

IV. THE REALITY OF THE REDSHIFT SYSTEMS

Clearly, because of the density of lines, one expects many systems to arise by chance. The reality of the redshifts can be examined by two different methods.

We will first make a statistical assessment of the overall significance of the identifications, and then we will examine the systems individually. Since the distribution of lines in wavelength is not uniform, the line list was divided into six 100 Å regions and the statistical tests were applied to each region separately: The expected number of chance C IV doublets in a region is given by

$$E(\text{C IV}) = \frac{N(N - 1)}{L} \times 2\Delta\lambda \times P,$$

where N is the number of lines in the region, L is the extent of the region in Å, $\Delta\lambda$ is the required accuracy

TABLE 5

STATISTICS OF C IV AND Si II IDENTIFICATIONS

REGION ($\lambda\lambda$)	No. OF LINES (N)	C IV DOUBLETS		N(Si II)	E_1	E_2	ACTUAL NUMBER OF Si II LINES		
		E(C IV)	Actual No.				$\lambda1526$	$\lambda1533$	Both Lines
3700–3800....	30	3.9 ± 1.8	2	1	0.2 ± 0.4	0.03 ± 0.17	1	0	0
3800–3900....	30	3.9 ± 1.8	4	6	1.1 ± 0.9	0.19 ± 0.43	3	2	2
3900–4000....	31	4.2 ± 1.9	6	8	1.5 ± 1.0	0.27 ± 0.51	3	3	2
4000–4100....	39	6.7 ± 2.4	13	22	5.2 ± 2.0	1.17 ± 1.05	11	7	4
4100–4200....	41	7.4 ± 2.5	15	5	1.2 ± 1.0	0.30 ± 0.53	1	2	1
4200–4300....	22	2.1 ± 1.4	5	1	0.1 ± 0.3	0.02 ± 0.14	0	1	0
Totals.....		28.2 ± 4.9	45		9.3 ± 2.6	1.98 ± 1.37	19	15	9

of the separation, and P is the probability of fulfilling the relative equivalent-width criterion by chance. Taking $L = 100$, $\Delta\lambda = 0.3$, and $P = 0.75$, we evaluated E(C IV) for each region; the results are given in Table 5. We see from this table that over the whole wavelength region $\lambda\lambda3700$–4300 we expect 28.2 ± 4.9 C IV doublets to be found by chance, whereas in fact there are 45 such systems. Both the expected number of C IV doublets E(C IV) and the excess over chance show a peak in the wavelength interval $\lambda\lambda4000$–4200. Here there are 28 observed systems, whereas 14.1 ± 3.5 are expected by chance.

A similar method was used to determine the significance of the Si II $\lambda\lambda1526$, 1533 identifications. In that case,

$$E_1 = N(\text{Si II}) \times \frac{2N\Delta\lambda}{L},$$

$$E_2 = N(\text{Si II}) \times \frac{2N\Delta\lambda}{L} \times \frac{2(N-1)\Delta\lambda}{L},$$

where E_1 is the expected number of identifications of one of the Si II lines in a region, E_2 is the expected number of identifications of both Si II lines in a region, and N(Si II) is the number of C IV redshifts for which the Si II lines are expected to occur in the region. The results of these calculations are also given in Table 5. The expected number of chance identifications of a single line, E_1, is 9.3 ± 2.6, and the expected number of chance identifications of two lines, E_2, is 1.98 ± 1.37 over the whole wavelength range.

Significant excesses of identifications of the individual lines and both lines exist. There are 19 identifications of Si II $\lambda1526$, 15 of the $\lambda1533$ line, and nine of both lines. These correspond to a 3.7 σ excess for the $\lambda1526$ line, a 2.2 σ excess for the $\lambda1533$ line, and a 5.1 σ excess for both lines. There is also a tendency for the systems with strong C IV lines to show the Si II $\lambda1526$ line; although only 40% of all systems have Si II $\lambda1526$ identifications, 70% of the 14 systems in which C IV $\lambda1548$ has an equivalent width greater than 0.4 Å have a Si II $\lambda1526$ identification.

We have divided the redshifts into three groups according to our estimate of their likelihood of being real. These groups are indicated in the last column of Table 3, in which C indicates a certain system, PR a probable system, and PO a possible system. All of the certain systems, 1.5023, 1.5950, 1.5964, 1.6102, 1.6556, 1.6568, 1.6581, 1.6703, 1.6714, 1.6732, and 1.6747, were given a high estimate of plausibility because of the strength of the C IV doublets. Moreover, all but one of these C IV doublets occur in the spectral region $\lambda\lambda4000$–4200 in which there is the large statistical excess of such doublets.

Most of the systems which have been labeled probable, 1.5153, 1.5348, 1.6399, 1.6598, 1.6599, 1.6820, and 1.6907, have been given this classification because they identify both Si II lines $\lambda\lambda1526$, 1533. Since there are nine such systems and only two are expected by chance, these have a high probability of being real. Two of the remaining systems, 1.5559 and 1.5603, have been labeled as probable because of the appearance of the C IV lines. While they are not very strong, the profiles indicate that there are several closely spaced C IV doublets at about $\lambda3960$. Three other redshifts, 1.5144, 1.6356, and 1.6365, have been called probable because of the lines other than C IV and Si II which are identified. The 1.5144 system convincingly identifies the Si IV doublet $\lambda\lambda1393$, 1403. The 1.6356 and 1.6365 systems (1.6365 was suggested by Boksenberg and Sargent as a doubtful system) identify the strongest line in that part of the spectrum shortward of the IPCS observations as $L\alpha$.

The remaining 22 redshifts are considered possible systems; they identify only C IV doublets and one or two other lines. An exception to this is the system at $z = 1.4007$, which identifies four strong lines. Two of these, however, are more convincingly identified in redshift systems designated as "certain."

V. DISCUSSION

a) The Distribution of Redshifts

The distribution in redshift of the 45 C IV systems is shown in Figure 5. Clearly, there is a peak in this distribution around $z_{\text{abs}} \approx 1.65$. Most of the systems that we have labeled as "certain" in Table 3 fall in this peak. If the absorption systems are due to intervening objects at cosmological redshifts, then the
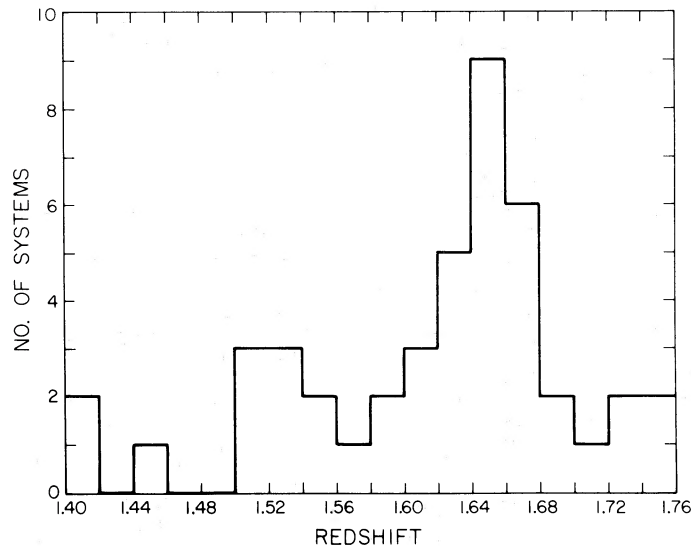
FIG. 5.—A histogram of the distribution in PKS 0237−23 of C IV doublets in redshift

existence of the peak in Figure 5 implies that these objects are not distributed uniformly. This can be shown formally as follows. If intervening material is distributed at random along the line of sight, Bahcall and Peebles (1969) have shown that their variable

$$X(z) = \int_0^z (1 + z)^2 [H_0/H(z)] dz ,$$

where

$$H(z) = \left\{ \frac{8}{3} \pi G \rho_0 (1 + z)^2 \left(z + \frac{1}{2q_0} \right) \right.$$
$$\left. - \frac{\Lambda}{3} \left[\frac{(1 + z)^2}{q_0} + z^2 + 2z \right] \right\}^{1/2}$$

is expected to be uniformly distributed. For $q_0 = \frac{1}{2}$ and $\Lambda = 0$, this gives $X(z) = 2/3[(1 + z)^{3/2} - 1]$. This can then be normalized by defining: $Y_i = [X(z_i) - X(z_l)]/[X(z_u) - X(z_l)]$ where z_u and z_l are the highest redshift and lowest redshift, respectively, for which one would expect to see the C IV doublet in these data ($z_u = 1.7651$, $z_l = 1.4007$). In this case, for which the number of redshifts allows conventional statistical tests to be used, a chi-square determination was made in order to compare the distribution of the 45 y_i's with a uniform random distribution between 0 and 1. The result of this test was that the chance that these redshifts represent intervening material at cosmological distances *randomly distributed along the line of sight* is less than one part in 10^3.

The peak at $z = 1.65$ in the distribution of redshifts has a width $c\Delta z/(1 + z)$ of about 5000 km s^{-1}. If the absorption is produced by intervening material unassociated with the QSO, a similar peak should occur in the distribution of absorption redshifts found in QSOs with $z_{em} > 1.7$ near PKS 0237−23 on the plane of the sky. We speculate that a cluster of

clusters of galaxies could produce this peak and that such a cluster would have an angular size on the order of 1°. One of us (W. L. W. S.) is undertaking a search for QSOs near PKS 0237−23 in order to test this hypothesis.

b) Splittings between Redshifts

Boksenberg and Sargent (1975) noted two strange features in the distribution of the separations between their redshift systems. In seven cases they found pairs of systems split by $\Delta v = c\Delta z/(1 + z) = 141 \pm 9$ km s^{-1}, and in four cases they found pairs of systems split by $\Delta v = 500$ km s^{-1}, the separation of the C IV doublet.

The C IV redshift systems in the new data were examined for significant splittings as follows. The velocity separations, Δv, were calculated between each pair of systems, and a histogram of the distribution is plotted in Figure 6. The shaded part of the plot gives the distribution of Δv for those systems we have labeled "certain" and "probable." Any preferred splitting will appear as a peak in the histogram.

The significance of peaks in the histogram can be roughly estimated in the following way. The distribution of splittings between elements of a uniform random sample is a constant over fairly small splittings. There is a cutoff at very small splittings owing to the finite resolution of the observations. We therefore approximate the expected distribution of splittings by zero splittings from 0 to 100 km s^{-1} and the average number of splittings above this. We also take the square root of the average number as the standard deviation of the number of splittings at each velocity. For all the systems, the expected number is then 4.0 ± 2.0; and for the certain and probable systems, it is 1.4 ± 1.2. These two expected distributions are indicated by the horizontal lines in Figure 6. Only
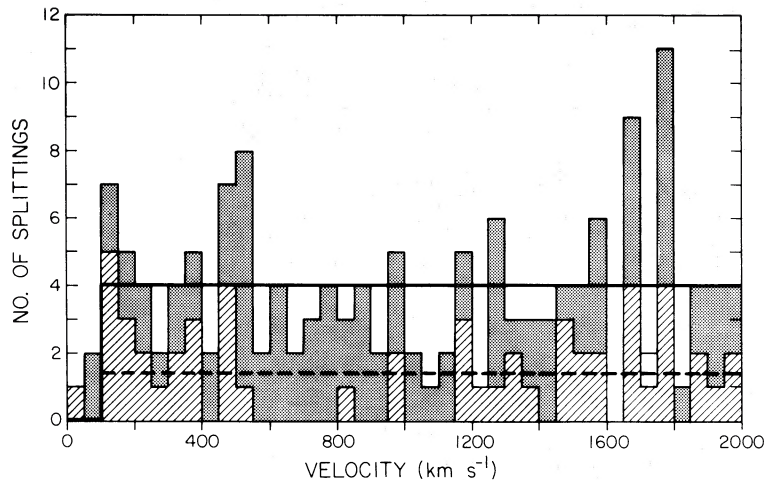
FIG. 6.—A histogram of all splittings $\Delta v = c\Delta z/(1 + z)$ of C IV redshift systems for $\Delta v \leq 2000$ km s^{-1}. The hatched portions show the distribution for the redshift systems defined by strong lines. The horizontal dashed line is the expected level for a flat distribution of splittings Δv. The shaded areas show the distribution of Δv for the weaker systems, as defined in the text. The solid horizontal line is the expected level for a flat distribution of splittings for all systems, strong and weak.

one peak in each distribution is 3 or more standard deviations above the expected curve. In the histogram of splittings between all systems there is a 3.5 σ excess of splittings between 1750 and 1800 km s^{-1}. Using the list of physically important line ratios λ_m/λ_n given by Burbidge and Burbidge (1975) and the criterion developed by Sargent and Boroson (1977) for the significance of such a comparison, namely,

$$\left| \frac{1 + z_1}{1 + z_2} - \frac{\lambda_m}{\lambda_n} \right| < 1.3 \times 10^{-4},$$

we find that, if this excess is produced by absorption-line locking, it can be due only to Lβ $\lambda1026$ and O VI $\lambda1031$.

In the distribution of splittings for the "certain" and "probable" systems, there is a peak between 100 and 150 km s^{-1} which is 3 σ above the expected level. Thus there is a real excess of small splittings in the distribution. This can be seen qualitatively from the spectrum itself, in which the systems occur in complexes; the scale of the structure in each complex is very much smaller than the separation between complexes.

Observations of the Mg II doublet at $z_{abs} = 0.424$ in the BL Lacertae object PKS 0735+178 have shown that at high resolution there are at least four redshifts separated by only 165 km s^{-1} in total (Boksenberg, Carswell, and Sargent 1978). This implies that there is no "magic splitting" in QSO absorption redshifts and that the peak at small splittings in PKS 0237−23 is due to a combination of instrumental resolution and a continuous distribution of splittings on a scale of at most $\sim$200 km s^{-1}. This possibility was suggested by Bahcall (1975). As mentioned by Bahcall, the velocity scale associated with the fine splittings is comparable with the scale expected for clouds in extended galactic halos. Moreover, Boksenberg and Sargent (1978) have shown that there is interstellar

gas containing heavy elements far out in the halo of at least one spiral galaxy, NGC 3067.

As can be seen from Figure 6, there is a marginal (2.5 σ) excess of splittings within the two bins adjacent to 498 km s^{-1}, corresponding to the C IV doublet separation, in the overall redshift distribution. In the distribution of the splittings for the "certain" and "probable" redshifts, there is an insignificant excess (1.3 σ) in these two bins. Accordingly, these new data give no strong confirmation that the C IV line locking suspected by Boksenberg and Sargent (1975) is real.

c) Si II Excited Fine-Structure Lines

The Si II $\lambda1533.44$ excited fine-structure transition gives an indication of some of the physical conditions in the absorbing cloud (Bahcall 1967; Bahcall and Wolf 1968). The ratio of the equivalent widths of the excited fine-structure and ground-state lines ($\lambda\lambda1533$, 1527) gives either the electron density of the cloud or the distance of the cloud from the continuum source, depending on whether the excited fine-structure level is collisionally or radiatively populated. In § IV we showed that a very significant excess of the C IV absorption systems have associated Si II lines $\lambda1526$ and $\lambda1533$. Thus we can say with confidence that some absorption redshifts in PKS 0237−23 with $0.5 \lesssim (z_{em} - z_{abs}) \lesssim 0.8$ have excited fine-structure Si II lines. Consequently, several of the clouds responsible for the absorption redshifts between 1.4 and 1.7 must have electron densities of order 10^3 cm^{-3} or greater. We know of no intergalactic objects which contain gas with a density as high as 10^3 cm, except for the dense gas clouds in the disks of spiral galaxies. Those, however, do not present a sufficiently large cross section to account for the number of observed systems with Si II excited fine-structure lines. On the other hand, the ejection hypothesis leads to difficulties with the systems which show the ground-state line but not

the excited fine-structure line. An example of this type of system is the "certain" system $z = 1.6714$, in which Si II $\lambda1526$ has an equivalent width of 1.1 Å and Si II $\lambda1533$ is not seen. Using the formula for collisional excitation to the fine-structure level derived by Bahcall (1967), we find that the electron density in the absorbing cloud must be $n_e \lesssim 50$ cm^{-3}. Under the assumption that the absorbing gas is ionized by the QSO, this upper limit can be combined with a parameter representing the ionization state of the system to give a lower limit on the distance scale of the cloud from the QSO (McKee, Tarter, and Weisheit 1973). For the $z = 1.6714$ system we take γ, the ionization parameter used by McKee et al., to be 10^4. We then find, from their equation (6), $r > 157$ kpc. This distance implies a mass of $2.5 \times 10^{10} M_\odot$ for the system if it is a complete shell and has a column density $n = 10^{19}$ cm^{-2}. An energy of $10^9 M_\odot c^2$ would be required to eject such a system; certainly this magnitude of mass and energy outflow is implausibly large, particularly in that it explains only a single system.

VI. CONCLUSIONS

New, high-resolution (0.7 Å) observations of the QSO PKS 0237−23 have been made with the university College London IPCS at the coudé focus of the Hale telescope. We have produced a list of 193 absorption lines in the wavelength range $\lambda3700$ to $\lambda4300$. An analysis of these lines leads to the following conclusions:

a) The autocorrelation function shows that the lines probably fall into two rest wavelength regions, one around Lα and one around the C IV doublet.

b) A search for C IV doublets has turned up 45 pairs of lines with the correct separation and intensity ratio. An examination of the individual systems leads us to designate 11 of the systems as "certain," 12 as "probable," and 22 as "possible."

c) A significant number of the redshifts show the excited fine-structure line $\lambda1533$ of Si II.

d) About 90 absorption lines remain unidentified; we believe that those shortward of the Lα emission line are probably identified as Lα with some N V, Si III, and Si II.

e) The distribution in redshift of the 45 C IV doublets is not uniform: there is a significant peak in the distribution at $z_{abs} \approx 1.65$ with a width $c\Delta z/(1 + z)$ of about 5000 km s^{-1}.

f) An examination was made of the distribution of splittings $\Delta v = c\Delta z/(1 + z)$ between redshifts up to $\Delta v = 2000$ km s^{-1}. There is a significant excess of splittings less than 200 km s^{-1} among the more certain redshifts. For all the systems, there is a 3.5σ excess of splittings at $\Delta v \approx 1800$ km s^{-1}. If this is due to absorption-line locking, then the only physical line pair which could account for it is Lβ and O VI $\lambda1031$. The new data show no significant evidence for C IV line locking.

g) If the lines are caused by intervening objects, then the results summarized in (c) and (e) imply that they must be nonuniformly distributed on a large scale and have high densities. On the other hand, the ejection hypothesis leads to an implausibly large mass and energy outflow from the QSO due to the systems which show the ground-state line but not the excited-structure line.

REFERENCES

Aaronson, M., McKee, C. F., and Weisheit, J. C. 1975, Ap. J., 198, 13.
Arp, H. C., Bolton, J. G., and Kinman, T. 1967, Ap. J., 147, 841.
Bahcall, J. N. 1967, Ap. J. (Letters), 149, L7.
———. 1968, Ap. J., 153, 679.
———. 1975, Ap. J. (Letters), 200, L1.
Bahcall, J. N., and Peebles, P. J. E. 1969, Ap. J. (Letters), 156, L7.
Bahcall, J. N., and Wolf, R. A. 1968, Ap. J., 152, 701.
Boksenberg, A., and Sargent, W. L. W. 1975, Ap. J., 198, 31.
———. 1978, Ap. J., 220, in press.
Boksenberg, A., Carswell, R. F., and Sargent, W. L. W. 1978, in preparation.
Burbidge, E. M., and Burbidge, G. R. 1975, Ap. J., 202, 287.
Goldreich, P., and Sargent, W. L. W. 1976, Comm. Astr. Ap., 6, 133.
McKee, C. F., Tarter, C. B., and Weisheit, J. C. 1973, Ap. Letters, 13, 13.
Sargent, W. L. W., and Boroson, T. A. 1977, Ap. J., 212, 383.

A. Boksenberg and R. F. Carswell: Department of Physics and Astronomy, University College London, Gower Street, London WC1E 6BT, England

Todd Boroson: Steward Observatory, University of Arizona, Tucson, AZ 85721

Wallace A. Sargent: Department of Astronomy 105-24, California Institute of Technology, Pasadena, CA 91125